High performance iPP based nanocomposites for food packaging application

M. Avella, M.E. Errico, G. Gentile

Istituto di Chimica e Tecnologia dei Polimeri, ICTP-CNR
Via Campi Flegrei, 34 Pozzuoli (NA), Italy, mave@ictp.cnr.it

ABSTRACT

High performance iPP based nanocomposites filled with innovative calcium carbonate nanoparticles ($CaCO_3$) were prepared and structure-properties relationships investigated. In particular nanoparticles characterized by high specific surface area (>200 m^2/g) and elongated shape were tested as reinforcement nanophase. In order to promote polymer/nanofillers interactions, $CaCO_3$ were coated with two different surface modifiers, polypropylene-maleic anhydride graft copolymer (iPP-g-MA) or fatty acids (FA). Morphological analysis permitted to assess that the presence of iPP-g-MA promotes a stronger adhesion between polymer/$CaCO_3$ with respect to that achieved by using FA as surface modifier. Mechanical analysis evidenced that Young's modulus increases as a function of nanoparticles content and coating agent nature. Finally, it was observed that the $CaCO_3$ nanoparticles presence drastically reduces the iPP permeability to both oxygen and carbon dioxide.

Keywords: nanocomposites, polypropylene, barrier properties, interfacial adhesion, mechanical properties.

1   INTRODUCTION

Isotactic polypropylene (iPP) is one of the most widely used plastic materials in the food packaging field [1]. Unfortunately polypropylene shows high gas permeability, which results in a poor protection of the packaged food thus limiting its usage [2]. One of the most used methods to improve polypropylene drawbacks is to add a second component such as a polymer in blend or in multilayer, micrometric fillers etc [3, 4]. Nowadays, nanocomposites based on polypropylene matrix constitute a major challenge for industry since they represent the route to substantially improve iPP mechanical and physical properties [5-7]. The enhanced properties are presumably due to the synergistic effects of nanoscale structure and interaction of fillers with polymers.

In this research, high performance iPP based nanocomposites filled with low-cost innovative calcium carbonate nanoparticles ($CaCO_3$) were prepared and structure-properties relationships investigated. Peculiarities of the innovative tested nanoparticles are the very high specific surface area (>200 m^2/g) and the elongated shape. This latter aims to merge the advantages of the well-assessed $CaCO_3$ know-how [8-11] with the properties enhancement attainable, for instance, by addition of clay platelets. In fact, in this way it should be possible to simulate the nanoclay behavior, that reduces gas permeability of polymers according to a tortuous path model, in which the platelets obstruct the passage of gases and other permeants through the polymeric matrix. Moreover, in order to promote polymer/nanofillers interfacial adhesion, $CaCO_3$ coated with polypropylene-maleic anhydride graft copolymer (iPP-g-MA) or fatty acids (FA) as surface modifiers were tested.

Structure-properties relationships were studied performing morphological, mechanical analysis and barrier tests.

2   EXPERIMENTAL SESSION

2.1   Materials

Isotactic polypropylene (iPP), Moplen X 30 S (Mn = 4.69×10^4 g/mol, Mw = 3.5×10^5 g/mol and Mz = 2.06×10^6 g/mol) was kindly supplied by Basell Polyolefins (Ferrara-Italy).

Elongated $CaCO_3$ nanoparticles (250 nm in length and 50 nm in thickness) coated with two different coupling agents, polypropylene-maleic anhydride graft copolymer (iPP-g-MA) and fatty acids (FA) were kindly supplied by Solvay Advanced Functional Minerals (Giraud-France). Nanoparticles are coded as C-PPMA and C-FA respectively

2.2   Methods

iPP/$CaCO_3$ nanocomposites were prepared by mixing the components in a Brabender-like apparatus (Rheocord EC of HAAKE Inc., New Jersey, USA) at 200°C and 32 rpm for 10 min. The mixing ratios of iPP/CaCO3 (wt/wt) were: 100/0, 99/1, 97/3.

Plain iPP and iPP/$CaCO_3$ nanocomposites were successively compression-molded in a heated press at 200°C for 2 min without any applied pressure. After this period, a pressure of 100 bar was applied for 3 min, then the press platelets were rapidly cooled to room temperature by cold water. Finally, the pressure was released and the mold removed from the plates

Morphological analysis was performed by using a scanning electron microscope (SEM), Cambridge Stereoscan microscope model 440, on cryogenically fractured surfaces. Before the observation, samples were covered with a gold layer.

Tensile tests were performed on dumb-bell specimens (4 mm wide and 15 mm long) by using an Instron machine (model 5564) at room temperature and a cross-head speed of 10 mm/min. Young Modulus (E) was calculated from these curves in accordance to the ASTM D256 standard (average 10 samples tested).

Permeability tests were performed in a gas-membrane-gas instrument based on measurement of the downstream pressure increase at a constant upstream side-driving pressure. The apparatus and experimental procedures were similar to those reported elsewhere [12-13]. In each experiment, sufficient time was allowed to ensure attainment of steady-state permeation. The measurements were carried out at a pressure of 1 atm and at a temperature of 30°C.

The permeability was computed from the slope of the linear, steady-state part of the curve representing the permeated gas volume as a function of time. The gas diffusivity was calculated from the 'time lag' determined from the intercept of the steady-state permeability curve on the abscissa.

3   RESULTS AND DISCUSSION

iPP based nanocomposites were prepared by melt mixing. Elongated $CaCO_3$ nanoparticles coated with iPP-g-MA or FA as surface modifier were tested as nanophase. Particular interest was focused on the influence of surface modifier nature on the polymer/nanoparticles interaction and consequently on the final material properties.

3.1   Morphological Analysis

In order to evaluate nanofiller dispersion into polymeric matrix and the interfacial adhesion between the two components, morphological analysis was performed on fractured surface of nanocomposites. As an example, SEM micrographs of nanocomposites containing 3% (wt/wt) of C-FA and C-PPMA are shown in figs. 1 and 2, respectively. As it is possible to observe, both C-FA and C-PPMA appear homogeneously dispersed into iPP allowing to affirm that organic surface modifiers prevent the nanoparticles agglomeration. Nevertheless, the strength of the polymer/nanoparticles interfacial adhesion depends upon the surface modifier nature. In fact in the case of C-FA nanoparticles, SEM micrograph reveals few areas in which debonding phenomena occurred after that a mechanical stress was applied, fig. 1. On the contrary, C-PPMA nanoparticles are completely welded to the iPP phase. This result underlines a stronger adhesion between polymer/C-PPMA with respect to that obtained by using C-FA nanoparticles. It can be hypothesized that the presence iPP-g-MA modifier agent is responsible for strong physical interactions between iPP-g-MA molecules and polymeric matrix entanglements. Interactions via entanglements can be only promoted if the molar mass of the surface modifier is quite high. It is known that the alkyl chains of fatty acids

are too short to interact with matrix chains via the above described mechanism. Nevertheless, the presence of fatty acids reduces the polarity and the absorption surface energy of nanoparticles preventing their agglomeration.
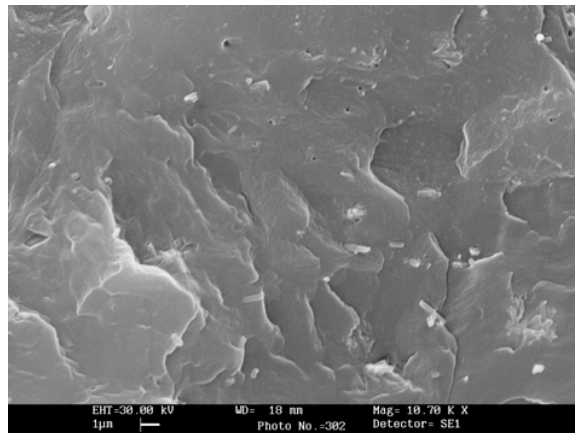

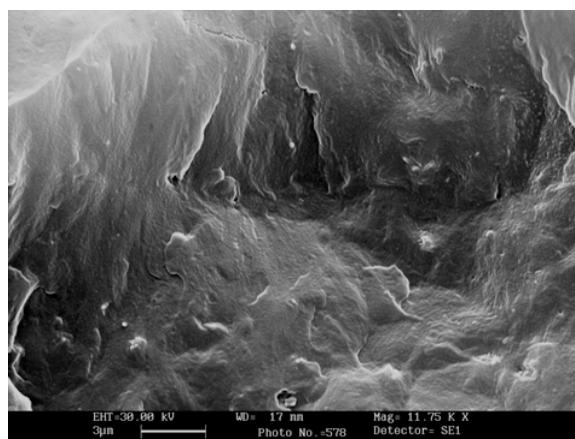Figure 1: SEM micrograph of iPP/ C-FA 3% (wt/wt) fractured surface.

Figure 2: SEM micrograph of iPP/ C-PPMA 3% (wt/wt) fractured surface.

3.2   Mechanical properties

Results of tensile tests performed on iPP based nanocomposites are resumed in fig. 3. As shown, the presence of nanoparticles increases Young's modulus and the extent of this improvement is strictly correlated to the surface modifier nature. In fact, $CaCO_3$ coated with iPP-g-MA gave rise to a more pronounced modulus increase up to 30% with respect to neat iPP value and almost 20% higher than those obtained with nanoparticles coated with FA. Moreover in the latter case the stiffness is slightly influenced by the filler content reaching the maximum

improvement by addition of 1% (wt/wt) of C-FA nanoparticles; while in the case of C-PPMA a dependence of modulus value up on the filler content was observed.

These results allow assessing that there is a significant influence of the interaction nature between filler particles and polymeric matrix on the iPP-based nanocomposites tensile properties. In fact, it is well known that in a multiphase system such as nanocomposites an external applied load can be transferred from the polymer to the reinforcement phase through the interphase region obtaining mechanical improvements as a function of the reached polymer/nanoparticles adhesion level. As above described, C-PPMA nanoparticles permit to obtain a better interfacial adhesion between the components (fig. 1) due to a strong surface modifiers-polymer interaction, assuring, in this way, a larger increase of the Young's modulus.
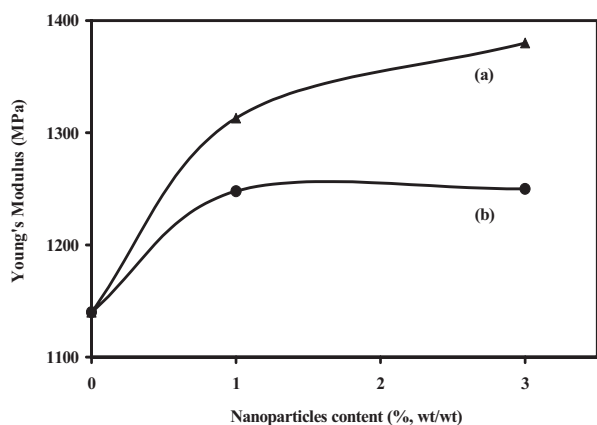

Figure 3: Young's Modulus values of iPP and iPP based nanocomposites filled with: a) C-FA nanoparticles; b) C-PPMA nanoparticles.

3.3 Barrier Properties

Generally speaking for an impermeable filler of volume fraction ϕ, the composite permeability (Pc) is directly linked to the tortuosity factor (τ) of nanoparticles, according to the following relationships [14]:

$$Pc = Pm \ (1- \phi)/\tau \tag{1}$$

$$\tau = 1 + (L/2W)\phi \tag{2}$$

where L and W denote the length and the thickness of the fillers and the ratio L/2W represents the aspect ratio.

In Figs. 4-5 oxygen and carbon dioxide permeability coefficient values versus nanoparticles content are plotted. As reported, C-FA and C-PPMA nanoparticles are responsible for a decrease of iPP permeability either to oxygen or to carbon dioxide. Moreover, the surface

modifier nature seems to play a key role in the extent of the iPP permeability improvement. In fact, while the C-FA nanoparticles lower the iPP permeability to oxygen up to 50% (fig. 4b), in the case of C-PPMA nanofillers this decrease is around 35% (fig. 4a). A similar trend was observed for the permeability to carbon dioxide as summarized in fig 5a-b. This result could be explained by considering that additional interactions generating between surface modifier (PP-g-MA or FA) and either oxygen or carbon dioxide occur. Although the C-PPMA nanoparticles induce a stronger C-PPMA/iPP interfacial adhesion, the nature of the surface modifier is similar to that of the polymeric matrix such as their permeability properties to oxygen and carbon dioxide. As a matter of fact, barrier properties are influenced only by the tortuous path that diffusing molecules must bypass with a consequent improvement of polymer permeability .

As far as C-FA nanoparticles, fatty acids unsaturations can be considered as potential sites of interactions with both oxygen and carbon dioxide molecules, thus inducing the additional effect of hindering and slowing the diffusion of the gases through the nanocomposites.

In a previous work, it was demonstrated that spherical $CaCO_3$ nanoparticles also induce an improvement of iPP barrier properties, due to the high nanoparticles volume fraction occupied, the homogeneous $CaCO_3$ dispersion and the strong matrix-nanofiller interfacial adhesion reached [11]. However, the relevance of this phenomenon is less pronounced with respect to that discussed in this work.

As a matter of fact, it can be assessed that elongated nanoparticles permit to magnify the well known effect of $CaCO_3$ spherical nanoparticles on the permeability properties, in agreement with the equations (1) and (2) above reported.
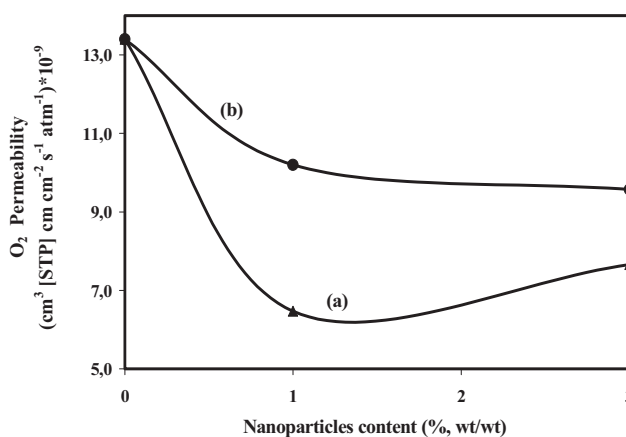

Figure 4: Oxygen permeability of iPP and iPP based nanocomposites filled with: a) C-FA nanoparticles; b) C-PPMA nanoparticles.
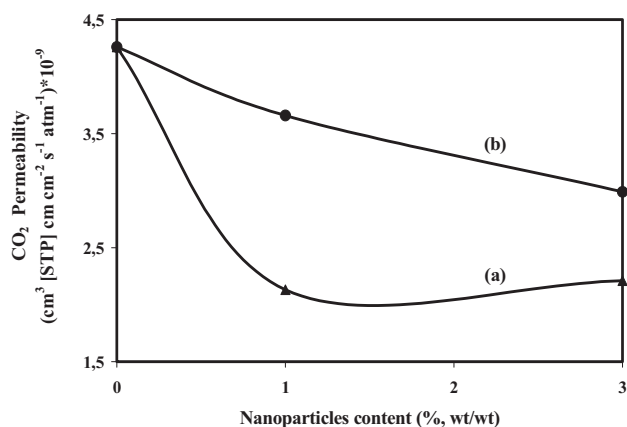
Figure 5: Carbon dioxide permeability of iPP and iPP based nanocomposites filled with: a) C-FA nanoparticles; b) C-PPMA nanoparticles

4 CONCLUSION

iPP based nanocomposites filled with innovative calcium carbonate nanoparticles were prepared and characterized. $CaCO_3$ nanoparticles were coated with two different surface modifiers, polypropylene-maleic anhydride graft copolymer (iPP-g-MA) or fatty acids (FA). The presence of the surface modifier prevents nanoparticles agglomeration phenomena allowing homogeneous dispersion of the nanophase into polymeric matrix. A close relationship between the surface modifier nature and final properties of the material was evidenced. Young's modulus increases in presence of nanoparticles. C-PPMA are responsible for a more pronounced improvement of iPP stiffness with respect to that achieved by addition of C-FA, due to stronger physical interactions between surface modifier and polymer via entanglements. $CaCO_3$ drastically reduces the iPP permeability to both oxygen and carbon dioxide because of nanoparticles elongated shape and good iPP/$CaCO_3$ interfacial adhesion. C-FA nanoparticles permit to obtain a larger effect on the barrier properties due probably to the presence of unsaturations that can be considered as potential sites of interactions with tested gases. These interactions induce the additional effect of hindering and slowing the diffusion of the gases through the nanocomposites.

REFERENCES

[1] J Karger Kocsis, "Polypropylene: structure, blends and composites" Chapman and Hall, 1995.

[2] H.G. Karian, "Handbook of polypropylene and polypropylene composites" Marcel Dekker, 1999.

[3] R.D. Deanin, M.A. Manion, "Handbook of Polyolefins" 2nd edition, Marcel Dekker, 633, 2000.

[4] M. Avella, P. Laurienzo, M. Malinconico, E. Martuscelli, M.G. Volpe, "Handbook of Polyolefins" 2nd edition, Marcel Dekker, 723, 2000.

[5] N. Hasegawa, H. Okamoto, M. Kato, A. Usuki, J. Appl. Polym. Sci 78 (11), 1918, 2000.

[6] E. Manias, A. Touny, L. Wu, K. Strawhecker, B. Lu, T.C. Chung, Chem. Mater. 13 (10), 3516, 2001.

[7] W.C.J. Zuiderluin, C. Westzaan, J. Huetink, R. J. Gaymans, Polymer 44(1), 261, 2003.

[8] M. Avella, M.E. Errico, E. Martuscelli, Nanoletters, 1(4), 213, 2001.

[9] M.L. Di Lorenzo, M.E. Errico, M. Avella, J Mater Sci 37(11), 2351, 2002.

[10] C.M. Chan, J. Wu, X. Li, Y.K. Cheung, Polymer 43(10), 2981-2992, 2002.

[11] M. Avella, S. Cosco, M.L. Di Lorenzo, E. Di Pace, M.E. Errico, G. Gentile European Polymer Journal in press.

[12] M.A. Del Nobile, G. Mensitieri , L. Nicolais, Polymer International 41, 73, 1996.

[13] L. Nicodemo, A. Marcone , T. Monetta, G. Mensitieri, F. Bellucci, J. Membrane Sci. 70, 207, 1, 1992.

[14] T.S. Ellis, J.S. D'Angelo, J. Appl. Polym. Sci. 90, 1639, 2003.